Self-diffusion in two-dimensional binary colloidal hard-sphere fluids

Alice L. Thorneywork,[1] Dirk G. A. L. Aarts,[1] Jürgen Horbach,[2] and Roel P. A. Dullens[1,*]

[1]*Department of Chemistry, Physical and Theoretical Chemistry Laboratory, University of Oxford, South Parks Road, Oxford OX1 3QZ, United Kingdom*

[2]*Institut für Theoretische Physik II, Heinrich-Heine-Universität Düsseldorf, Universitätsstrasse 1, 40225 Düsseldorf, Germany*

(Received 17 August 2016; published 31 January 2017)

We present a systematic experimental study of the dynamic behavior of monodisperse and bidisperse two-dimensional colloidal hard-sphere fluids. We consider the diffusive behavior of the two types of particles for systems with a variety of compositions and total area fractions. In particular, we measure the short- and long-time diffusion coefficients for both species independently. We find that the short-time self-diffusion coefficients show an approximately linear dependence on the area fraction and that the long-time self-diffusion coefficients are well described by an expression dependent upon only the area fraction and contact value of the radial distribution function. Finally, we consider the effect of composition change and find some variation in the long-time self-diffusion coefficients, which we ascribe to the complex packing effects exhibited by binary systems.

DOI: 10.1103/PhysRevE.95.012614

I. INTRODUCTION

Elucidating the relationship between the structural and dynamic properties of fluids has long been a problem [1–4], with, in recent years, particular effort toward understanding this link in the case of the glass transition [5–10]. Colloidal systems, which allow for the study of both the structure and dynamics at a single particle level in real time, play an important role in addressing condensed matter issues. For example, colloidal monolayers have been used to study melting phenomena [11–14], the properties of gels have been explored using colloid-polymer mixtures [15,16], and colloidal particles which are confined or subjected to external fields have been used to probe particle dynamics in complex landscapes [17–21]. In particular, binary colloidal systems, comprised of two differently sized components, are a popular model glass forming system [22–24] due to the required suppression of crystallization they afford. These binary systems, however, also exhibit interesting dynamical and structural phenomena away from the glass transition [25–27].

One of the simplest dynamical properties is the self-diffusion of particles, and numerous studies of this fundamental transport mechanism in three-dimensional (3D) colloidal systems, both monodisperse [4,28–31] and bidisperse [25,32–35], have been performed using both scattering techniques and confocal or optical microscopy. The dynamic properties of two-dimensional (2D) systems, and in particular of hard-disk systems, have also been the subject of many theoretical [36,37] and simulation [38–41] studies. For this case, the corresponding experimental realization is described as quasi-2D, consisting of a monolayer of particles with a 3D solvent, and a range of these systems, differing with respect to the interface and method of confinement, have been considered [3,40,42–57]. In the case of binary systems, however, the motivation to study the glassy behavior of the system has resulted in a focus on behavior at high area fractions [42,58].

The self-diffusion coefficient for a colloidal system at infinite dilution, D_0, in 3D is predicted to be [59]

$$D_0 = \frac{k_B T}{3\pi\eta\sigma}, \tag{1}$$

with η the viscosity of the solvent and σ the particle diameter. For two-dimensional systems this expression often requires modification to account for the method of confinement, for example by using Faxen's correction to describe the increased friction experienced by a particle close to a wall [60]. As the total area fraction, ϕ_t, of the system is increased, hydrodynamic and direct interactions between particles act to reduce the measured diffusion coefficient and introduce new time scales into the system [61]. As a result, two diffusion coefficients can be defined based upon the time scale over which the system is considered and the corresponding short- and long-time self-diffusion coefficients may be obtained from the particle dynamics in the limits of short and long times, respectively.

Even at relatively low packing fractions, direct and long-ranged hydrodynamic interactions make a full theoretical description of self-diffusion extremely complex [61]. In a previous study [62], however, we have shown that for our monodisperse colloidal system, the long-time self-diffusion coefficient scaled by D_0 is in excellent agreement with that from Monte Carlo simulations of hard disks. Crucially, these simulations do not include hydrodynamic interactions, implying that hydrodynamic interactions effectively do not affect the area-fraction dependence of the long-time self-diffusion coefficient in experiment. Therefore, it should be possible to describe the ϕ_t dependence of the long-time self-diffusion coefficient, also in binary fluids, using theoretical expressions that consider only the effect of direct interactions.

Here we study the short- and long-time self-dynamics of monodisperse and binary quasi-2D colloidal fluids, previously shown to structurally behave as hard-disk systems [63]. To achieve this we consider the variation of the long- and short-time self-diffusion coefficients over a wide range of compositions and area fractions. From these measurements we test the applicability of simple theoretical expressions to describe the observed behavior, where at long times we consider expressions which only consider direct interactions. As

*roel.dullens@chem.ox.ac.uk

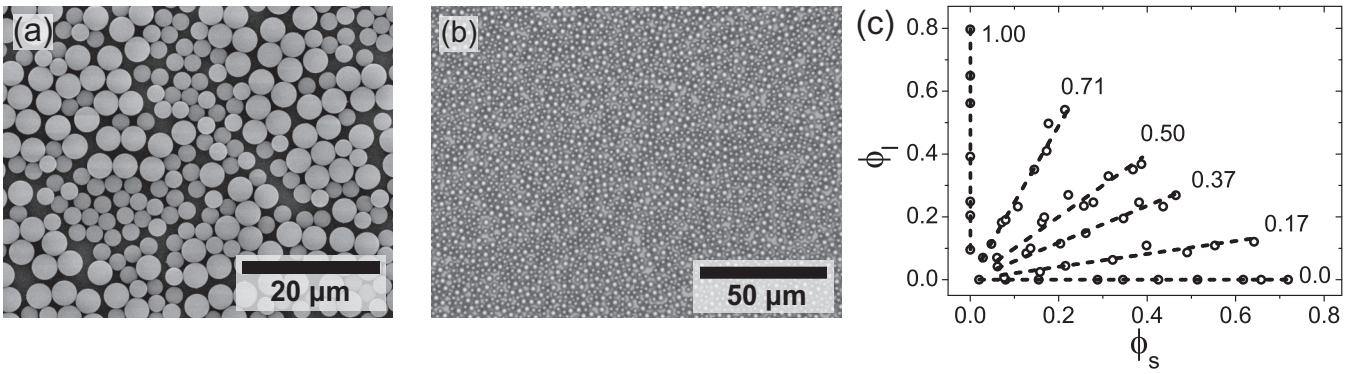

FIG. 1. (a) Scanning electron microscopy image of the (dried) binary colloidal mixture studied. (b) Typical optical microscopy image of a system at $q = 0.50$ and $\phi_t = 0.64$. (c) State diagram, from [63], showing the different system compositions studied, where the dashed lines denote systems of approximately the same composition, q.

such, we provide an extensive characterization of the dynamics of monodisperse and binary quasi-2D hard-sphere systems.

II. EXPERIMENTAL METHODS

A. Colloidal model system

The quasi-two-dimensional colloidal system, as introduced in Ref. [63], is composed of melamine formaldehyde particles (Microparticles GmbH) with hard-sphere diameters of $\sigma_s = 2.79$ and $\sigma_l = 4.04$ μm. Figure 1(a) shows an image from scanning electron microscopy of the binary mixture of particles, and Fig. 1(b) a typical optical microscopy image. The particles are dispersed in a 20/80 v/v% ethanol/water mixture and sediment onto the base of a glass sample cell to form monolayers of varying total area fraction, ϕ_t, where for binary systems $\phi_t = \phi_s + \phi_l$, with ϕ_s and ϕ_l the area fractions of the small and large particles, respectively. The gravitational lengths are 0.07 and 0.02 μm for the small and large particles, respectively, and thus out-of-plane fluctuations are negligible. The composition of the system is described by the parameter q, where $q = \phi_l/\phi_t$ with ϕ_l the area fraction of the large component. Six different systems with q values of approximately 0, 0.17, 0.37, 0.50, 0.71, and 1 are considered, such that we examine the full state space for binary systems, as shown in the state diagram in Fig. 1(c) (taken from [63]).

B. Video microscopy

The system is imaged at a rate of two frames per second for up to 45 min using a simple video-microscopy setup, consisting of an Olympus CKX41 inverted microscope with a 40× objective and equipped with a PixeLink CMOS camera (1280 × 1080 pixels). Standard particle tracking software [64] was used to obtain particle coordinates, with an error of 12 ± 10 nm in the particle position [63]. Typically between 3000 and 4000 particles per frame were found for the highest values of ϕ_t, with the large and small particles distinguished based upon the brightness of features.

C. Data analysis

The mean-squared displacement (MSD) is calculated from particle trajectories as

$$\delta r^2(t) = \langle [\mathbf{r}_i(t) - \mathbf{r}_i(0)]^2 \rangle, \tag{2}$$

with $\mathbf{r}_i(t)$ the position of particle i at time t and $\langle \dots \rangle$ the average over multiple particles and different time origins. For binary systems, the MSD is calculated separately for the subsets of small and large particles. The short- and long-time self-diffusion coefficients are determined from the initial and long-time behavior of the MSD as

$$D_S^{s,l} = \lim_{t\to 0} \frac{\delta r^2(t)}{4t} \text{ and } D_L^{s,l} = \lim_{t\to \infty} \frac{\delta r^2(t)}{4t}. \tag{3}$$

Here, the superscript denotes the type of particle (i.e., small s or large l) and the subscript denotes the type of diffusion (i.e., S for short time, L for long time). For each binary system studied, four diffusion coefficients may therefore be calculated; short-time diffusion for small particles (D_S^s), short-time diffusion for large particles (D_S^l), long-time diffusion for small particles (D_L^s), and long-time diffusion for large particles (D_L^l). Note that $D_0^{s,l}$ is the self-diffusion coefficient at infinite dilution.

III. RESULTS AND DISCUSSION

A. Monodisperse system

We first consider self-diffusion in monodisperse colloidal fluids of either small ($\sigma = 2.79$ μm) or large ($\sigma = 4.04$ μm) particles, corresponding to the lines $q = 0$ and $q = 1$ in Fig. 1(c). Note that here we reexamine the self-diffusion of the monodisperse systems, previously discussed in [62], to validate, for a well-understood system, the expressions we later use to consider the self-diffusion in binary fluids. The mean-squared displacement for a range of total area fractions at $q = 0$ is shown in Fig. 2(a). The MSD displays linear, diffusive regimes at short and long times, with the onset of a plateau at intermediate times for high area fractions [10,65]. Qualitatively, there is no difference in the behavior seen for the two differently sized systems.

Short- and long-time self-diffusion coefficients were obtained from the initial and long-time slopes of the MSD [Eq. (3)] and are shown as a function of the total area fraction in Fig. 2(b). For both the small and large particles, the short- and long-time self-diffusion coefficients decrease with ϕ_t consistent with the increased hindrance to the motion of the particles as the area fraction increases [61]. An estimate of D_0 is obtained by an extrapolation of the measured self-diffusion

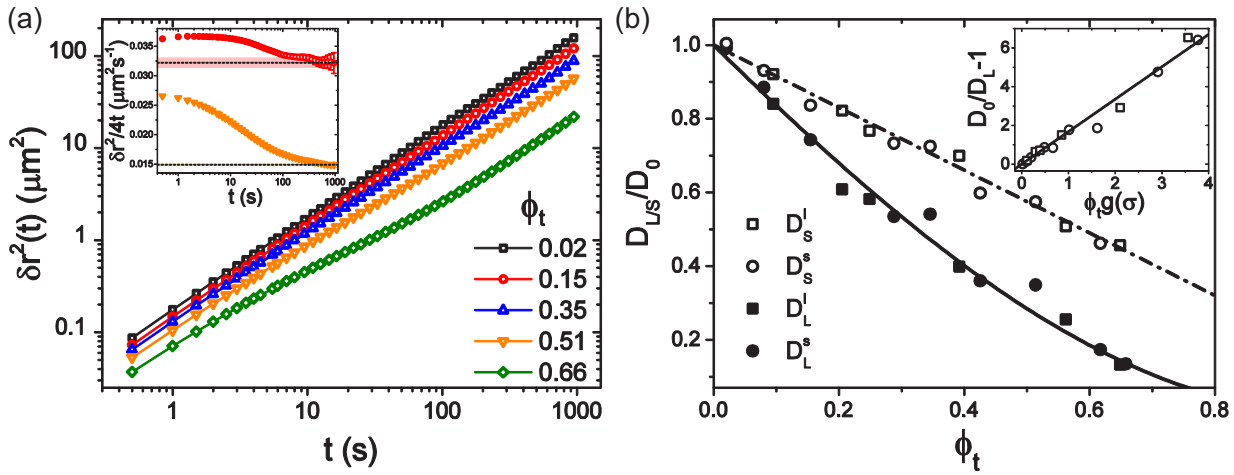

FIG. 2. (a) Mean-squared displacements of monodisperse systems of 2.79 μm particles ($q = 0$) at various ϕ_t. Inset is the approach of the function $\delta r^2/4t$ to its limiting long-time value for $\phi_t = 0.15$ and 0.51. Here the black dashed line indicates the value of D_L, and the shaded region the mean error in the MSD in the long-time limit. (b) Diffusion coefficients for the monodisperse small and large particle systems, scaled by the diffusion coefficient at infinite dilution, D_0 (see Table I). The dashed line shows the prediction for the short-time diffusion coefficient from Eq. (4) with $\alpha = 0.85$ and the solid line the prediction for the long-time diffusion coefficient from Eq. (5) with $\beta = 1.675$. Inset is the linear fit from Eq. (6) used to compute β.

coefficients at low ϕ_t to $\phi_t = 0$ and these values for the monodisperse systems, i.e., $q = 0$ and 1, are shown in Table I. The extrapolated values vary slightly, but are consistent with the value of D_0 as predicted by Eq. (1) when the presence of the wall is accounted for by Faxen's correction [60]. We estimate a maximum uncertainty in the value of the diffusion coefficients of approximately $\pm 3\%$ by considering the approach of $\delta r^2/4t$ to its limiting value at long times. Typical examples of the behavior of this function at two values of ϕ_t are shown in the inset to Fig. 2(a). Here, black dashed lines indicate the value of D_L and the shaded region represents the mean error on the MSD in the long-time limit, where the long-time limit is defined to include all points for which D_L lies within the error bar of the MSD.

At low area fractions, the short-time diffusion coefficient is expected to vary linearly with ϕ_t [28,31,66,67] as

$$\frac{D_S}{D_0} = 1 - \alpha\phi_t. \tag{4}$$

For our monodisperse systems, the area fraction dependence of D_S was discussed previously in [62], with the values of α, determined from a linear fit, found to be 0.87 ± 0.06 and 0.84 ± 0.04 for the small and large systems, respectively. This fit, with an average value of $\alpha = 0.85$, is shown in Fig. 2(b), and is in good agreement with our data, even at relatively high area fractions. These values of α are lower than that predicted in 3D [68], consistent with previous studies of quasi-2D systems [48,49,69].

TABLE I. Experimental values of the self-diffusion coefficients at infinite dilution ($D^{s/l}_{0,S/L}$), determined by an extrapolation of the short- and long-time diffusion coefficients for small and large particles to $\phi_t = 0$. Diffusion coefficients are measured in $\mu m^2\,s^{-1}$ and for a range of compositions q.

q	$D^s_{0,S}$	$D^s_{0,L}$	$D^l_{0,S}$	$D^l_{0,L}$
0.00	0.0438	0.0420		
0.17	0.0411	0.0363	0.0260	0.0249
0.37	0.0460	0.0420	0.0274	0.0251
0.50	0.0561	0.0478	0.0339	0.0274
0.71	0.0466	0.0405	0.0289	0.0250
1.00			0.0266	0.0267

The change of the long-time self-diffusion coefficient with ϕ_t is expected to be more complex as this may be dependent on both hydrodynamic and direct interactions, though there is no consensus as to how hydrodynamic interactions affect D_L [41,52,54,70–73]. In spite of this, we have previously shown that for our colloidal system at long times the behavior is in excellent agreement with results from Monte Carlo simulations of hard disks, which importantly do not include hydrodynamic interactions [62]. As such, we now compare the long-time behavior to simple theoretical expressions, which describe only the effect of direct interactions on the self-diffusion coefficient. The term accounting for direct interactions is expected to depend sensitively on the structure of the system and has been described by an expression of the form [2,29,37,74]

$$D_L = \frac{D_0}{1 + \beta\phi_t g(\sigma)}, \tag{5}$$

where $g(\sigma)$ is the contact value of the radial distribution function and β a constant. Theoretical studies suggest that $\beta = 2$ in both 3D [2,29,74] and 2D [37] consistent with analyses considering the area fraction dependence of the long-time self-diffusion coefficient to first order in ϕ_t [75,76]. In spite of this, in 2D the expression has been seen to fail for higher area fractions, requiring the use of additional terms from mode-coupling theory to describe the behavior [37].

To test the applicability of a purely structural expression of the form of Eq. (5) to describe D_L over the entire range of ϕ_t, we rewrite Eq. (5) as

$$\frac{D_0}{D_L} - 1 = \beta\phi_t g(\sigma), \tag{6}$$

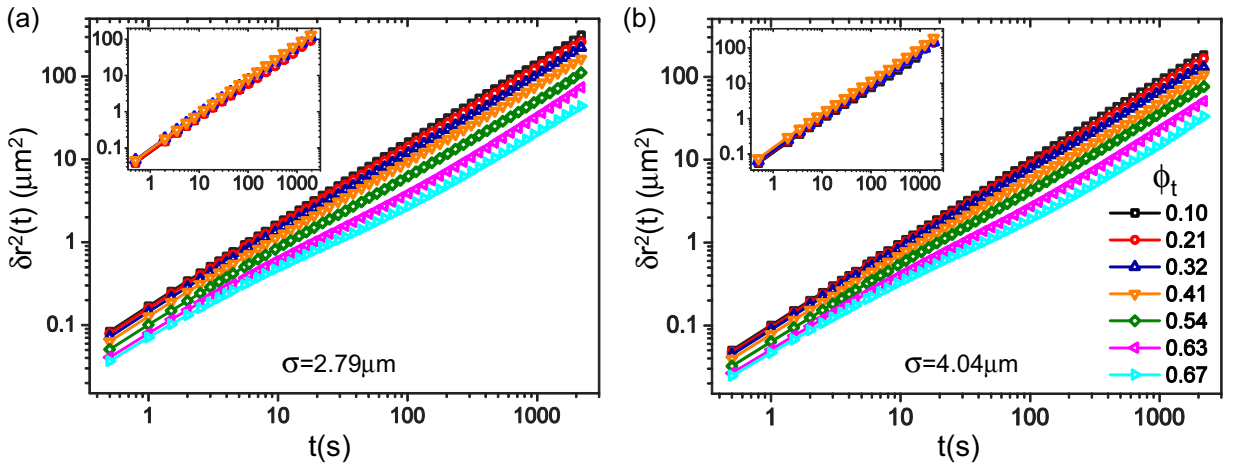

FIG. 3. Mean-squared displacement of (a) small and (b) large particles in a binary system with composition $q = 0.37$. Values of ϕ_t in panel (b) refer to both plots. Insets show the MSD for (a) small and (b) large particles in systems of varying composition, $q = 0 \rightarrow 1$, but an approximately constant area fraction of $\phi_t = 0.4$.

and fit this expression to our experimental data. Here, β is a constant to be determined and $g(\sigma)$ the expression for the contact value from scaled particle theory [77], which we have previously shown to describe $g(\sigma)$ very well for our system [63]. The resultant linear fits produce values of $\beta = 1.62 \pm 0.06$ for the 2.79 μm system and $\beta = 1.73 \pm 0.09$ for the 4.04 μm system. A comparison of the experimental data to Eq. (6) with an averaged value of $\beta = 1.675$ is shown in the inset of Fig. 2(b), where linear behavior is seen across the whole range of area fractions. The value of β as measured from our experiments is somewhat different to the value of 2 expected from theory, but while the origin of this difference in the value of β is unclear, we find that the general form of Eq. (6) describes the experimental data well. We show the comparison between the experimental long-time self-diffusion coefficient and Eq. (5) in Fig. 2(b) and – as expected from the linear fit to Eq. (6) – good agreement is seen over the whole range of densities for both monodisperse systems. With our experimental data we therefore demonstrate the applicability of a simple expression, Eq. (5), that directly links the structure and long-time dynamics in the system. It should be noted however, that if the prediction of Eq. (5) is compared to the simulation in [62], it provides a good estimate of D_L at low and intermediate area fractions, but shows different qualitative behavior at high ϕ_t.

B. Binary system

Next, we consider the particle dynamics in binary colloidal hard-sphere fluids. To this end, we first plot the MSD for both the small and large particles in a binary system for fixed composition of $q = 0.37$ and increasing total area fraction in Fig. 3. As for the monodisperse case, the MSD has linear regimes at short and long times and shows clearly the onset of subdiffusive behavior at high ϕ_t. The same qualitative behavior is seen for both the small and large particles for all compositions considered. It is also possible to compare the MSD for binary systems of the same total area fraction but with different compositions and these results are shown as insets in Figs. 3(a) and 3(b) for $\phi_t \approx 0.4$ and compositions $q = 0 \rightarrow 1$. This comparison is more difficult, because our sample preparation method makes it difficult to fix ϕ_t. Consequently, we see approximately the same behavior for the small and large particles across the state diagram, with small variations in total area fraction obscuring any differences in the MSD due to the composition change.

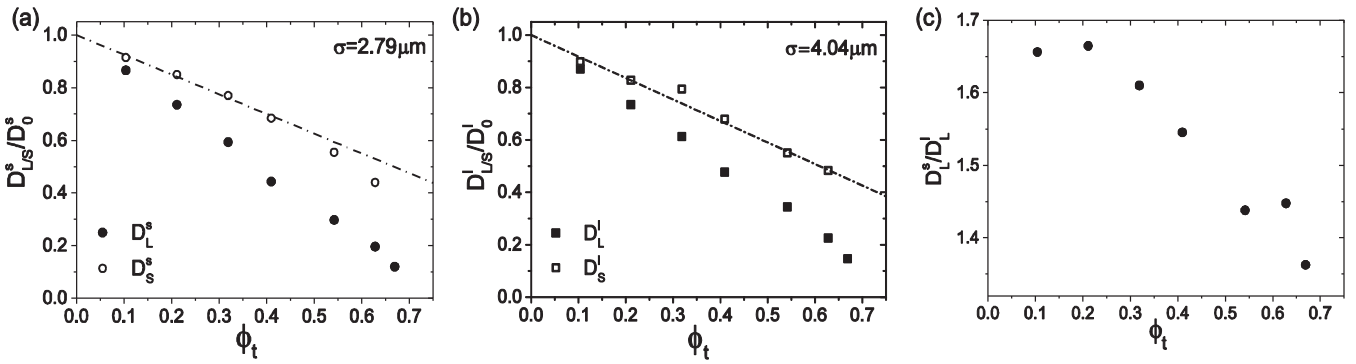

FIG. 4. Short- and long-time self-diffusion coefficients for (a) small and (b) large particles in a binary system at $q = 0.37$. Filled circles show the long-time self-diffusion coefficient and open circles the short-time self-diffusion coefficients, with the dashed line from Eq. (4) with $\alpha = 0.8$ in (a) and $\alpha = 0.75$ in (b). The ratio of the long-time self-diffusion coefficients for the large and small particles is shown in (c).

TABLE II. Experimental values of α and β for the small and large particles in the binary systems for different compositions q and for the two monodisperse systems ($q = 0$ and 1).

q	α_s	α_l	β_s	β_l
0.00	0.87 ± 0.06		1.62 ± 0.06	
0.17	0.69 ± 0.09	0.73 ± 0.10	1.35 ± 0.04	1.13 ± 0.06
0.37	0.75 ± 0.05	0.82 ± 0.04	1.32 ± 0.01	1.01 ± 0.02
0.50	0.91 ± 0.07	0.93 ± 0.07	1.43 ± 0.05	1.08 ± 0.04
0.71	0.85 ± 0.10	0.80 ± 0.08	1.17 ± 0.03	0.90 ± 0.04
1.00		0.84 ± 0.04		1.73 ± 0.09

In Fig. 4 we show the short- and long-time self-diffusion coefficients for the small and large particles as a function of ϕ_t for the binary system with $q = 0.37$. For all systems the self-diffusion coefficient decreases with increasing total area fraction, as seen for the monodisperse system. The extrapolated values for D_0 for the small and large particles for short- and long-time self-diffusion are similar to those for the monodisperse systems, see Table I, with all values consistent with the Einstein expression [Eq. (1)] when corrected for the presence of the wall [60]. From the short-time self-diffusion coefficient, we again obtained the values of α for the large and small particles, which are presented in Table II for the four compositions considered. Here, it can be seen that values of α for large and small particles in systems of the same composition are very similar and that all values of α are within error of that of the monodisperse systems.

Consistent with D scaling inversely with the particle size [Eq. (1)], the values of D_L and D_S are greater for the small particles than those of the large particles in a binary system at a certain area fraction and composition. However, as ϕ_t increases there appears to be a convergence in the values of D_L for the two different particle sizes, suggesting that at high area fractions the diffusive behavior is dictated to a lesser extent by the particle size. This can be seen in the variation of the ratio of the long-time self-diffusion coefficients for the small and large particles, as shown in Fig. 4(c), where the value becomes closer to unity with increasing ϕ_t. While the value of this ratio at low ϕ_t is consistent with the ratio of the D_0 values for the small and large particles (see Table I), it does not exactly correspond to the size ratio. We believe this may be due to the effect of slightly different Faxen's corrections for the small and large particles.

We now again attempt to describe the long-time self-diffusion coefficient in the binary fluids using an expression that only accounts for direct interactions. We consider an ansatz for mixtures of particles based upon Eq. (5),

$$\frac{D_L^i}{D_0^i} = \frac{1}{1 + \beta_i \phi_t [x_i g_{ii}(\sigma_{ii}) + x_j g_{ij}(\sigma_{ij})]}, \tag{7}$$

where i, j indicates particle identity, i.e., small or large, $x_{i,j} = N_{i,j}/N$ is the number fraction of small or large particles, and $g_{ij}(\sigma_{ij})$ is the contact value of the partial radial distribution function with $\sigma_{ij} = (\sigma_i + \sigma_j)/2$. To account for mixtures of particles, we have expressed the structural dependence as a linear combination of the contact values of the partial radial distribution functions. These contact values are determined as for the monodisperse system and agree well with the theoretical expression [78] for $g_{ij}(\sigma_{ij})$ [63]. As with the monodisperse system, we calculate values of β by considering the linear fit that arises from a rearrangement of Eq. (7). Unlike the values of α, values of β are systematically larger for the small particles (see Table II), with an example of the linear fits for the $q = 0.37$ system shown in the inset of Fig. 5.

A comparison between the experimental long-time self-diffusion coefficients and Eq. (7) for small and large particles at all four compositions is shown in Fig. 5. Here, D_L^i is plotted against ϕ_i to better demonstrate the quality of the agreement. In general the experimental data are well described by Eq. (7). Since this expression only considers the effect of direct interactions on D_L^i, this agreement also suggests that the convergence in the long-time self-diffusion coefficients of the two differently sized particles at high area fraction [Fig. 4(c)] arises from the complex packing effects seen in binary systems [79].

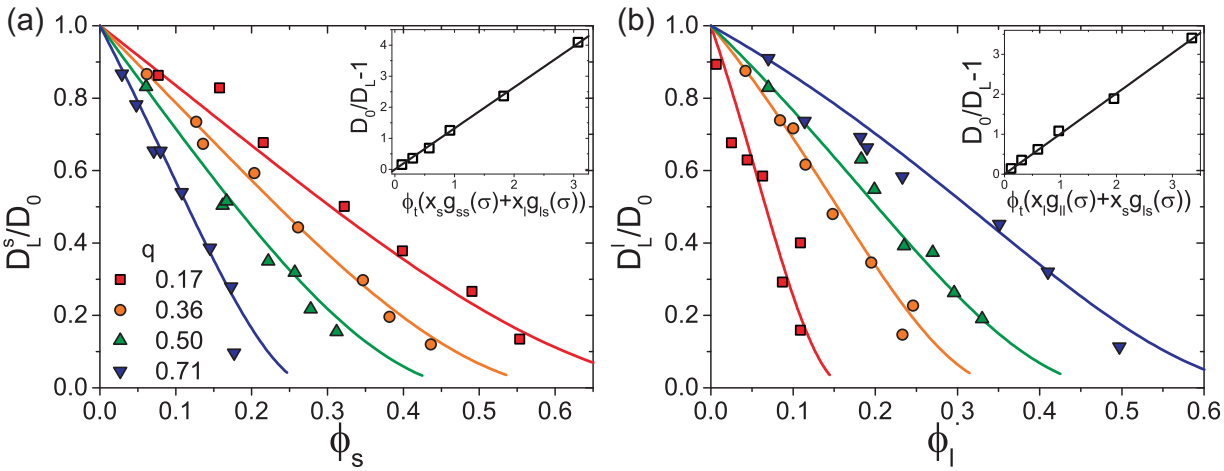

FIG. 5. Long-time self-diffusion coefficients for the four binary systems for (a) small and (b) large particles with the prediction from Eq. (7). Here, self-diffusion coefficients for each component are plotted against the area fraction of that component for clarity. Inset is an example of the linear plot used to calculate β for the (a) small and (b) large $q = 0.37$ systems.

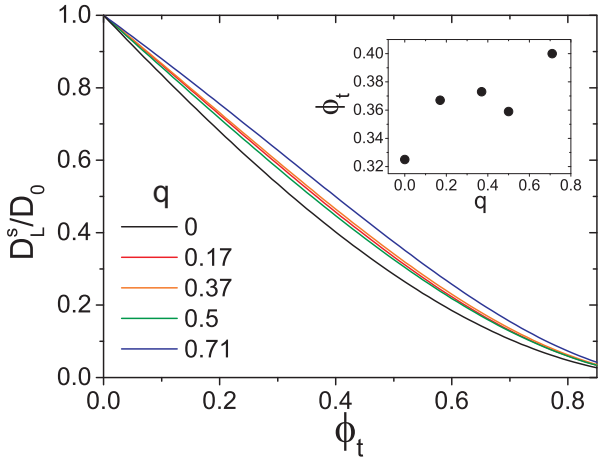

FIG. 6. D_L^s/D_0 as obtained from Eq. (7) using the experimentally determined values of β (see Table II) for small particles in a binary system. Here the expression is plotted as a function of ϕ_t to demonstrate the variation with composition q. Inset is the total area fraction at which the scaled long-time self-diffusion coefficient, D_L^s/D_0, is equal to 0.5.

It was not possible to see significant composition dependence of the MSD (Fig. 3) due to the difficulty in preparing systems with varying q but sufficiently similar ϕ_t. A comparison of the fits to the D_L^i data shown in Fig. 5, however, does allow small composition effects on D_L^i to be probed. Consequently, in Fig. 6 we show Eq. (7) computed with the values of β for the small particles in the monodisperse ($q = 0$) and binary ($q \neq 0$) systems. Additionally, the inset of Fig. 6 shows how the value of ϕ_t at which the scaled long-time self-diffusion coefficient, D_L^s/D_0, is equal to 0.5, varies with composition. Note that similar results are obtained for the large particles (data not shown). Notably, in all four binary systems the long-time self-diffusion coefficients are larger than in a monodisperse system of the same area fraction. The exact effect of composition change, however, is not clear, although the system which exhibits the fastest self-diffusion is that with approximately equal numbers of large and small particles. The complex dependence on composition seen here is consistent with previous studies of structural relaxation in binary systems [79], where properties were seen to depend upon the composition and exact size ratio in an extremely complex manner.

IV. CONCLUSIONS

We have systematically studied the self-dynamic behavior of quasi-2D binary colloidal hard-sphere fluids over a wide range of total area fractions and a variety of compositions. Mean-squared displacements show the expected behavior with increasing ϕ_t for a system approaching the onset of the glass transition. The short- and long-time self-diffusion coefficients for both the small and large particles decrease with increasing area fraction as the motion of the particles becomes more hindered. However, at high area fractions the values of the long-time self-diffusion coefficients for small and large particles appear to converge. Both the short- and long-time self-diffusion coefficients can be well approximated by simple expressions in terms of the total area fraction. In particular, the long-time behavior can be described by considering only the effect of direct interactions using a relationship based on the structure of the system, consistent with our previous work [62]. Finally, the long-time self-diffusion coefficients in binary systems exhibit a mild composition dependence related to the structure and packing within the system.

ACKNOWLEDGMENTS

We thank Thomas Skinner and Michael Juniper for useful discussions. We thank the EPSRC, ERC (ERC Starting Grant 279541-IMCOLMAT), DFG research unit FOR-1394 "Nonlinear response to probe vitrification" (HO 2231/7-2), and the Royal Society for financial support.

[1] J. Rallison, J. Fluid Mech. **186**, 471 (1988).
[2] J. F. Brady, J. Fluid Mech. **272**, 109 (1994).
[3] X. Ma, W. Chen, Z. Wang, Y. Peng, Y. Han, and P. Tong, Phys. Rev. Lett. **110**, 078302 (2013).
[4] P. Holmqvist and G. Nägele, Phys. Rev. Lett. **104**, 058301 (2010).
[5] T. Kawasaki and H. Tanaka, J. Phys.: Condens. Matter **23**, 194121 (2011).
[6] A. Widmer-Cooper, P. Harrowell, and H. Fynewever, Phys. Rev. Lett. **93**, 135701 (2004).
[7] L. Berthier and W. Kob, Phys. Rev. E **85**, 011102 (2012).
[8] D. N. Perera and P. Harrowell, Phys. Rev. Lett. **81**, 120 (1998).
[9] E. R. Weeks and D. A. Weitz, Phys. Rev. Lett. **89**, 095704 (2002).
[10] W. Kegel and A. van Blaaderen, Science **287**, 290 (2000).
[11] C. A. Murray and D. H. Van Winkle, Phys. Rev. Lett. **58**, 1200 (1987).
[12] R. P. A. Dullens and C. Bechinger, Phys. Rev. Lett. **107**, 138301 (2011).
[13] K. Zahn, R. Lenke, and G. Maret, Phys. Rev. Lett. **82**, 2721 (1999).
[14] Y. Han, N. Y. Ha, A. M. Alsayed, and A. G. Yodh, Phys. Rev. E **77**, 041406 (2008).
[15] M. M. van Schooneveld, V. W. A. de Villeneuve, R. P. A. Dullens, D. G. A. L. Aarts, M. E. Leunissen, and W. K. Kegel, J. Phys. Chem. B **113**, 4560 (2009).
[16] C. P. Royall, S. R. Williams, T. Ohtsuka, and H. Tanaka, Nat. Mater. **7**, 556 (2008).
[17] T. O. E. Skinner, S. K. Schnyder, D. G. A. L. Aarts, J. Horbach, and R. P. A. Dullens, Phys. Rev. Lett. **111**, 128301 (2013).
[18] F. Evers, C. Zunke, R. D. L. Hanes, J. Bewerunge, I. Ladadwa, A. Heuer, and S. U. Egelhaaf, Phys. Rev. E **88**, 022125 (2013).
[19] M. P. N. Juniper, A. V. Straube, R. Besseling, D. G. A. L. Aarts, and R. P. A. Dullens, Nat. Commun. **6**, 7187 (2015).
[20] M. P. N. Juniper, A. V. Straube, D. G. A. L. Aarts, and R. P. A. Dullens, Phys. Rev. E **93**, 012608 (2016).

[21] X.-G. Ma, P.-Y. Lai, B. J. Ackerson, and P. Tong, Soft Matter **11**, 1182 (2015),
[22] T. Narumi, S. V. Franklin, K. W. Desmond, M. Toluyama, and E. R. Weeks, Soft Matter **7**, 1472 (2011).
[23] H. König, R. Hund, K. Zahn, and G. Maret, Euro. Phys. J. E. **18**, 287 (2005).
[24] K. H. Nagamanasa, S. Gokhale, A. K. Sood, and R. Ganapathy, Nat. Phys. **11**, 403 (2015).
[25] P. D. Kaplan, A. G. Yodh, and D. J. Pine, Phys. Rev. Lett. **68**, 393 (1992).
[26] K. Kim, K. Miyazaki, and S. Saito, Europhys. Lett. **88**, 36002 (2009).
[27] J. Baumgartl, R. P. A. Dullens, M. Dijkstra, R. Roth, and C. Bechinger, Phys. Rev. Lett. **98**, 198303 (2007).
[28] R. Ottewill and N. Williams, Nature **325**, 232 (1987).
[29] A. van Blaaderen, J. Peetermans, G. Maret, and J. K. G. Dhont, J. Chem. Phys. **96**, 4591 (1992).
[30] W. van Megen, S. M. Underwood, and I. Snook, J. Chem. Phys. **85**, 4065 (1986).
[31] X. Qiu, X. L. Wu, J. Z. Xue, D. J. Pine, D. A. Weitz, and P. M. Chaikin, Phys. Rev. Lett. **65**, 516 (1990).
[32] A. Imhof and J. K. G. Dhont, Phys. Rev. E **52**, 6344 (1995).
[33] G. D. J. Phillies, J. Chem. Phys. **81**, 1487 (1984).
[34] R. Krause, G. Nägele, J. Arauz-Lara, and R. Weber, J. Colloid Interface Sci. **148**, 231 (1992).
[35] S. R. Williams and W. van Megen, Phys. Rev. E **64**, 041502 (2001).
[36] D. M. Gass, J. Chem. Phys. **54**, 1898 (1971).
[37] J. Schofield, A. H. Marcus, and S. A. Rice, J. Phys. Chem. **100**, 18950 (1996).
[38] R. García-Rojo, S. Luding, and J. J. Brey, Phys. Rev. E **74**, 061305 (2006).
[39] W.-S. Xu, Z.-Y. Sun, and L.-J. An, J. Chem. Phys. **137**, 104509 (2012).
[40] E. Falck, J. M. Lahtinen, I. Vattulainen, and T. Ala-Nissila, Euro. Phys. J. E **13**, 267 (2004).
[41] R. Pesche and G. Nagele, Phys. Rev. E, **62**, 5432 (2000).
[42] S. Mazoyer, F. Ebert, G. Maret, and P. Keim, Europhys. Lett. **88**, 66004 (2009).
[43] J. Santana-Solano and J. L. Arauz-Lara, Phys. Rev. E **65**, 021406 (2002).
[44] J. Santana-Solano, A. Ramírez-Saito, and J. L. Arauz-Lara, Phys. Rev. Lett. **95**, 198301 (2005).
[45] M. D. Carbajal-Tinoco, G. Cruz de León, and J. L. Arauz-Lara, Phys. Rev. E **56**, 6962 (1997).
[46] A. H. Marcus, B. Lin, and S. A. Rice, Phys. Rev. E **53**, 1765 (1996).
[47] B. Cui, B. Lin, and S. A. Rice, J. Chem. Phys. **114**, 9142 (2001).
[48] W. Chen and P. Tong, Europhys. Lett. **84**, 28003 (2008).
[49] Y. Peng, W. Chen, T. M. Fischer, D. A. Weitz, and P. Tong, J. Fluid Mech. **618**, 243 (2008).
[50] P. Holmqvist, J. K. G. Dhont, and P. R. Lang, Phys. Rev. E **74**, 021402 (2006).
[51] P. P. Lele, J. W. Swan, J. F. Brady, N. J. Wagner, and E. M. Furst, Soft Matter **7**, 6844 (2011).
[52] K. Zahn, J. M. Méndez-Alcaraz, and G. Maret, Phys. Rev. Lett. **79**, 175 (1997).
[53] A. Ramírez-Saito, J. Santana-Solano, B. Bonilla-Capilla, and J. L. Arauz-Lara, J. Non-Newton. Fluid **165**, 941 (2010).
[54] B. Cui, H. Diamant, B. Lin, and S. A. Rice, Phys. Rev. Lett. **92**, 258301 (2004).
[55] B. Bonilla-Capilla, A. Ramírez-Saito, M. A. Ojeda-López, and J. L. Arauz-Lara, J. Phys.: Condens. Matter **24**, 464126 (2012).
[56] A. L. Thorneywork, D. G. A. L. Aarts, J. Horbach, and R. P. A. Dullens, Soft Matter **12**, 4129 (2016).
[57] E. Sarmiento-Gomez, J. R. Villanueva-Valencia, S. Herrera-Velarde, J. A. Ruiz-Santoyo, J. Santana-Solano, J. L. Arauz-Lara, and R. Castañeda-Priego, Phys. Rev. E **94**, 012608 (2016).
[58] F. Ebert, P. Keim, and G. Maret, Eur. Phys. J. E **26**, 161 (2008).
[59] J.-P. Hansen and I. Mcdonald, *Theory of Simple Liquids* (Academic, New York, 2006), 3rd ed.
[60] J. Leach, H. Mushfique, S. Keen, R. Di Leonardo, G. Ruocco, J. M. Cooper, and M. J. Padgett, Phys. Rev. E **79**, 026301 (2009).
[61] J. K. G. Dhont, *An Introduction to Dynamics of Colloids* (Elsevier, New York, 1996).
[62] A. L. Thorneywork, R. E. Rozas, R. P. A. Dullens, and J. Horbach, Phys. Rev. Lett. **115**, 268301 (2015).
[63] A. L. Thorneywork, R. Roth, D. G. A. L. Aarts, and R. P. A. Dullens, J. Chem. Phys. **140**, 161106 (2014).
[64] J. Crocker and D. Grier, J. Colloid Interface Sci. **179**, 298 (1996).
[65] E. R. Weeks, Science **287**, 627 (2000).
[66] W. van Megen and S. M. Underwood, J. Chem. Phys. **91**, 552 (1989).
[67] M. M. Kops-Werkhoven, J. Chem. Phys. **74**, 1618 (1981).
[68] G. K. Batchelor, J. Fluid Mech. **131**, 155 (1983).
[69] V. N. Michailidou, G. Petekidis, J. W. Swan, and J. F. Brady, Phys. Rev. Lett. **102**, 068302 (2009).
[70] A. H. Marcus, J. Schofield, and S. A. Rice, Phys. Rev. E **60**, 5725 (1999).
[71] J. Bleibel, A. Domínguez, F. Günther, J. Harting, and M. Oettel, Soft Matter **10**, 2945 (2014).
[72] R. Pesché, M. Kollmann, and G. Nägele, J. Chem. Phys. **114**, 8701 (2001).
[73] R. Pesché and G. Nägele, Europhys. Lett. **51**, 584 (2000).
[74] J. A. Leegwater and G. Szamel, Phys. Rev. A **46**, 4999 (1992).
[75] B. J. Ackerson, J. Chem. Phys. **76**, 2675 (1982).
[76] H. N. W. Lekkerkerker and J. K. G. Dhont, J. Chem. Phys. **80**, 5790 (1984).
[77] E. Helfand, H. L. Frisch, and J. L. Lebowitz, J. Chem. Phys. **34**, 1037 (1961).
[78] A. Santos, S. B. Yuste, and M. López de Haro, J. Chem. Phys. **117**, 5785 (2002).
[79] W. Götze and T. Voigtmann, Phys. Rev. E **67**, 021502 (2003).